Population-averaged age-specific DTI templates of preterm human brain at 33, 36 and 39 gestational weeks

Virendra Mishra[1], Kenichi Oishi[2], Hang Li[1,3], Tina Jeon[1], Minhui Ouyang[1], Lina Chalak[4], Jonathan M Chia[5], Yun Peng[3], Nancy Rollins[6], Susumu Mori[2], and Hao Huang[1,7]

[1]Advanced Imaging Research Center, University of Texas Southwestern Medical Center, Dallas, Texas, United States, [2]Department of Radiology and Radiological Science, The Johns Hopkins University School of Medicine, Baltimore, Maryland, United States, [3]Department of Radiology, Beijing Children's Hospital Affiliated to Capital Medical University, Beijing, China, [4]Department of Pediatrics, University of Texas Southwestern Medical Center, Dallas, Texas, United States, [5]Philips Medical Systems, Dallas, Texas, United States, [6]Department of Radiology, Children's Medical Center at Dallas, Dallas, Texas, United States, [7]Department of Radiology, University of Texas Southwestern Medical Center, Dallas, Texas, United States

Target audience: MR physicist, pediatric neurologist, pediatric radiologist and neonatologist.

Purpose: From 30 weeks of gestation (wg) to normal time of birth (40wg), human brain maturation results in dramatic structural alterations [e.g. 1-3], that include not only microstructural changes such as disappearance of organized radial glial scaffold in the cortical plate, but also macrostructural changes of brain shape, size and morphology. These dramatic structural differences make it difficult and presumably inaccurate to adopt a single atlas for MRI and DTI acquired from preterm brains in the age range of 30wg to 40wg. Recently, age-specific templates based on T2 contrasts [2,4] were established covering the age range of 30wg to 40wg. However, except a DTI atlas for term neonate brains [5], no population-averaged age-specific DTI template at 33wg, 36wg and 39wg is available. In this study, we aimed to establish population-averaged age-specific DTI templates of preterm human brains at 33wg, 36wg and 39wg. We further evaluated these age-specific DTI templates by showing statistically significant and inhomogeneous local expansions with transformations of younger preterm brains to the templates of older brains.

Methods: *Subjects:* 72 recruited preterm and term neonates with the age range of 31wg to 42wg at the scan time were divided into 3 age groups at 33wg, 36wg and 39wg as follows. 15 preterm neonates scanned at 31wg to 34.57wg (12M/3F, scan time age: 33.47±0.9wg), 30 preterm neonates scanned at 34.57wg to 37.57wg (18M/12F, scan time age: 36.06±0.84) and 27 preterm or term neonates scanned at 37.57wg to 42.0wg (19M/8F, scan time age: 39.91±1.16) were categorized into 33wg, 36wg and 39wg group, respectively. All subjects were normal after rigorous screening procedures conducted by the neonatologist and pediatric radiologist. *DTI data acquisition:* All neonates were well fed before scanning and kept asleep during scan. DTI was acquired from a 3T Philips Achieva MR system with SS-EPI and SENSE parallel imaging (SENSE factor=2.5). The diffusion MRI imaging parameters were: TE=78ms, TR=6850ms, in-plane field of view = 168x168mm^2, in-plane imaging resolution=1.5x1.5mm^2, slice thickness=1.6mm, slice number=60, 30 independent diffusion-weighted directions [6], b-value = 1000 sec/mm^2, repetitions=2. The axial diffusion MRI image dimension was zero-filled to 256x256 after reconstruction. The total acquisition time for DTI was 11 minutes. Diffusion tensor was fitted with *DTIStudio*. DTI-derived metrics including fractional anisotropy (FA) maps and color-encoded orientation maps were also obtained with *DTIStudio*. *Establishment of age-specific DTI templates at 33wg, 36wg and 39wg:* The diffusion tensor and the b0 images of each subject were resampled to get the volume data with isotropic resolution of 0.6x0.6x0.6mm^3. The six-step procedures for generating the JHU-neonate atlas [5] were applied to datasets in each age group to establish 3 population-averaged age-specific templates at 33wg, 36wg and 39wg, respectively. Briefly, these 6 steps include one step of AC-PC alignment, one step of direct averaging of images, three consecutive steps of affine transformations and one last step of dual-channel LDDMM transformation [7]. All transformations were conducted with *DiffeoMap* software (mristudio.org). After transformations, co-registered b0, FA and tensor were averaged to generate population-averaged age-specific b0 and DTI template. *Evaluation of age-specific DTI templates:* 5 random subjects (4M/1F, scan time age: 33.34±0.97wg) from the 33wg age group were chosen to evaluate the 3 population-averaged age-specific DTI templates. Each of the 5 subjects was registered to 3 age-specific single subject (SS) template using dual-channel LDDMM transformation with FA and MD driving the transformation. Note that the 33wg SS template was regenerated for evaluation following the protocol [5] after exclusion of these 5 subjects. 3 sets of transformation matrices were created corresponding to 3 SS template at 33wg, 36wg and 39wg, respectively. Based on these transformation matrices, the Jacobian determinants [e.g. 8] quantifying the local expansion and contraction were calculated.

Results: *Population-averaged age-specific DTI templates:* Population-averaged age-specific linear, nonlinear and SS b0 images, FA maps and colormaps at the 33wg, 36wg and 39wg are demonstrated in Fig 1. As pointed by the yellow arrows in the FA maps, high cortical FA shown as a bright band in the cortical plate can be clearly observed at younger ages of 33wg and 36wg. However, this bright cortical band is no longer visible at 39wg. Besides clear microstructural changes, remarkable macrostructural changes in terms of shape, size and morphology of the brains across 3 time points are shown in Fig. 1. *Evaluation of the age-specific DTI templates:* The Jacobian maps overlaid on top of the SS b0 template image at 33wg, 36wg and 39wg are shown in Fig. 2a. From Fig. 2a, higher local volume expansions (Jacobian determinant greater than 1) were found in frontal and temporal areas with the target template at 36wg and 39wg. The mean Jacobian determinants increase with the age increase of the target brain at 33wg (green), 36wg (blue) and 39wg (red), shown in Fig. 2b. Fig. 2c shows that the center of the Jacobian histogram with the transformation to 33wg SS template brain is close to 1 and centers of the Jacobian histograms with the transformations to 36wg and 39wg SS template brains shift to the value of 1.2.

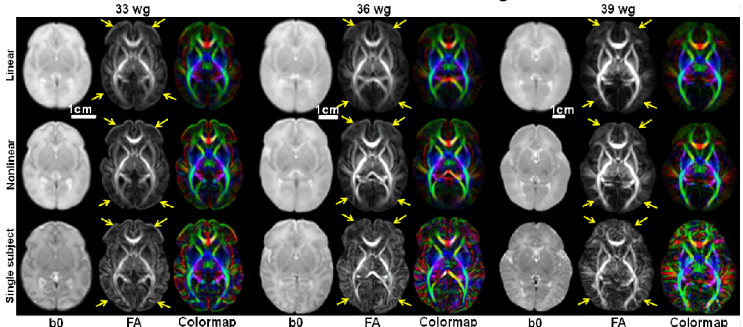

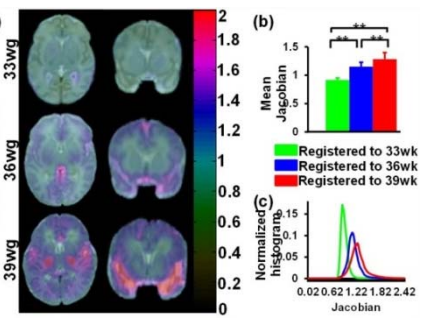

Fig 1 (left): Population-averaged linear (top panels), nonlinear (middle panels) and single subject (lower panels) b0 images, FA maps and colormaps at 33wg, 36wg and 39wg from left to right.

Fig 2 (right): (a) Jacobian map on top of the 33wg, 36wg and 39wg SS b0 template; (b) Mean and standard deviation of the Jacobian with transformation to 33wg (green), 36wg (blue) and 39wg (red) SS b0 template; (c) Normalized Jacobian histogram showing distribution of the Jacobian determinant values with transformations to 33wg (green), 36wg (blue) and 39wg (red) SS b0 template. Color bar in (a) encodes Jacobian values. **: p<0.001.

Discussion and Conclusion: In this study, we have generated population-averaged age-specific DTI templates of preterm and term human brains at 33wg, 36wg and 39g. Both microstructural and macrostructural changes are dramatic, as shown in Fig. 1. The evaluation with Jacobian measurements demonstrated statistically significant and inhomogeenous local expansions with transformation of the younger brains to the template of older brains. These results suggest that the age-specific DTI templates at three time points could potentially enhance accuracy of normalization of the preterm brains from 30wg to 40wg, and improved normalization could potentially increase sensitivity in detecting structural abnormality of pathological preterm brains. Further evaluations of the templates with DTI eigenvector coherence are underway. **References:** [1] Huang et al. (2006) Neuroimage 33: 27. [2] Kuklisova-Murgasova et al. (2011) Neuroimage 54: 2750. [3] Ball et al (2014) PNAS 110: 9541. [4] Serag et al. (2012) Neuroimage 59: 2255. [5] Oishi et al. (2011) Neuroimage 56: 8. [6] Jones et al (1999) MRM 32: 515. [7] Ceritoglu et al. (2009) Neuroimage 47: 618. [8] Gaser et al. (2001) Neuroimage 13:1140. ***Acknowledgement:*** This study is sponsored by NIH MH092535 and MH092535-S1.